Kinematics and strain distribution of a thrust-related fold system in the Lewis thrust plate, northwestern Montana (U.S.A.)

AN YIN and GERHARD OERTEL

Department of Earth and Space Sciences, University of California, Los Angeles, CA 90024-1567, U.S.A.

Abstract—In order to understand interactions between motion along thrusts and the associated style of deformation and strain distribution in their hangingwalls, geologic mapping and strain measurements were conducted in an excellently exposed thrust-related fold system in the Lewis thrust plate, northwestern Montana. This system consists of: (1) an E-directed basal thrust (the Gunsight thrust) that has a flat–ramp geometry and a slip of about 3.6 km; (2) an E-verging asymmetric anticline with its nearly vertical forelimb truncated by the basal thrust from below; (3) a 4-km wide fold belt, the frontal fold complex, that lies directly in front of the E-verging anticline; (4) a W-directed bedding-parallel fault (the Mount Thompson fault) that bounds the top of the frontal fold belt and separates it from the undeformed to broadly folded strata above; and (5) regionally developed, W-dipping spaced cleavage. Although the overall geometry of the thrust-related fold system differs from any previously documented fault-related folds, the E-verging anticline itself resembles geometrically a Rich-type fault-bend fold. The observed initial cut-off and fold interlimb angles of this anticline, however, cannot be explained by cross-section balancing models for the development of either a fault-bend fold or a fault-propagation fold. Possible origins for the E-verging anticline include (1) the fold initiated as an open fault-bend fold and tightened only later during its emplacement along the basal thrust and (2) the fold started as either a fault-bend or a fault-propagation fold, but simultaneous or subsequent volume change incompatible with any balanced cross-section models altered its shape.

Strain in the thrust-related fold system was determined by the preferred orientation of mica and chlorite grains. The direction and magnitude of the post-compaction strain varies from place to place. Strains in the forelimb of the hangingwall anticline imply bedding-parallel thinning at some localities and thickening at others. This inhomogeneity may be caused by the development of thrusts and folds. Strain in the backlimb of the hangingwall anticline implies bedding-parallel stretching in the thrust transport direction. This could be the effect of bending as the E-verging anticline was tightened and transported across the basal thrust ramp. Strain measured next to the Gunsight thrust again indicates locally varying shortening and extension in the transport direction, perhaps in response to inhomogeneous friction on the fault or else to a history of alternating strain hardening and softening in the basal thrust zone.

INTRODUCTION

RECENT studies on interactions between motion along a thrust fault and the geometrical evolution of its hanging-wall structures have established numerous cross-section balancing models for fault-associated folds (Suppe 1983, Jamison 1987, Mitra 1990, Suppe & Medwedeff 1990, Erslev 1991). Each of these models assumes a specific deformational style and strain path and conservation of area. For example, Suppe's model (1983) for the geometrical development of a Rich-type fault-bend fold (Rich 1934) requires that the hangingwall be deformed by a uniform bedding-parallel simple-shear strain history and that the deformational style be parallel-folding with kink-fold geometry. In the Jamison (1987) model, the developing forelimb of a fault-bend or fault-propagation fold is uniformly thinned or thickened. Assumptions about the strain path and the deformational style at depth used in these models are generally difficult to test, because they refer to subsurface structures known only from seismic profiles and only limited drill-hole data (Suppe & Namson 1979, Yoos *et al.* 1991). To test these balanced cross-section models, systematic studies of several well-exposed natural examples are required in which strain distributions, deformation histories, geometries of hangingwall structures, and displacements and geometries of underlying

thrusts are well defined. The knowledge gained from these studies can then be used as a guide for interpreting incompletely exposed structures. The purpose of this paper is (1) to describe the geometry of one well-exposed thrust-related fold system in the Lewis thrust plate in Glacier National Park, Montana, (2) to document the strain distribution in it and (3) to present a kinematic model for its evolution.

GEOLOGIC SETTING

The study area is located in west-central Glacier National Park, Montana (Fig. 1). Structures mapped for this study are part of the late Cretaceous to early Tertiary Lewis thrust system of the southern Canadian Rocky and western Montana fold and thrust belt (Bally *et al.* 1966, Mudge & Earhart 1980, Price 1981, Mudge 1982, Yin & Kelty 1991a). The Lewis thrust carries middle Proterozoic strata over late Cretaceous strata with a slip of several tens of kilometers (Price 1981). The first-order structural configuration of the Lewis plate has long been treated as a simple syncline, the Akamina syncline (Fig. 1) (Dahlstrom 1970) that extends from North Kootenay Pass of southeastern British Columbia to Marias Pass of northwestern Montana (Ross 1959, Gordy *et al.* 1977). Recent studies of this thrust system in
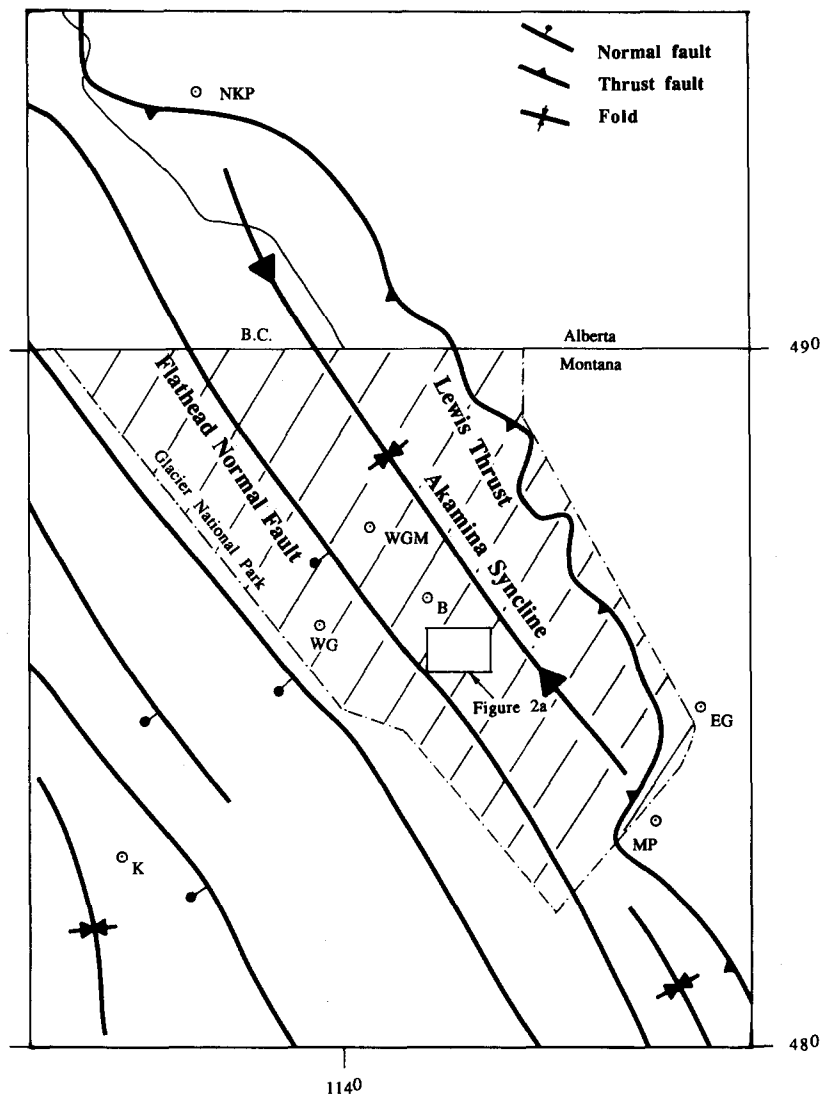
Fig. 1. Regional tectonic map of the Lewis thrust and the location of Fig. 2. B = Mount Brown; BC = British Colombia; WG = West Glacier; WGM = Wolf Gun Mountain; EG = East Glacier; MP = Marias Pass; NKP = North Kootenay Pass. Note that the Akamina syncline lies in the hangingwall of the Lewis thrust, and the study area Fig. 2 is located in the west limb of the syncline.

Glacier Park, Montana (Fig. 1) reveal that complex structures including duplexes, conjugate contraction faults, and normal faults lie underneath the little deformed Akamina syncline in the 2 km thick lower part of the 4.7 km thick Lewis plate (Davis & Jardine 1984, Yin & Davis 1988, Hudec & Davis 1989, Yin *et al*. 1989, Yin 1991, Yin & Kelty 1991a,b, Zarn 1991). In particular, Yin & Kelty (1991a) attributed the folding of the syncline to the development of two major duplex systems in the hangingwall of the Lewis thrust, the Rising Wolf duplex at the east side and the Brave Dog duplex at the west side of the park.

The stratigraphy of the Belt Supergroup in Glacier National Park has been described in detail by McGimsey (1979), Whipple *et al*. (1984), Jardine (1985), Kelty (1985), Hudec (1986) and Yin (1988). In the study area, it includes the Prichard, Appekunny, Grinnell, Empire, Helena and Snowslip Formations. The Prichard and Appekunny Formations consists exclusively of argillite. In the Grinnell Formation argillite and quartz arenite are interbedded. The Empire Formation consists of interbedded argillite, quartz arenite and limestone. The

Helena Formation is composed mainly of limestone with minor argillite. The Snowslip formation is composed of interbedded argillite, limestone, and quartz arenite. The abundance of argillite and the lack of other strain markers in the Belt strata make exploitation of the March theory (March 1932, Oertel 1983, 1985) the only available technique for strain determination.

STRUCTURAL GEOLOGY

Figure 2 is a simplified geologic map of the study area. Although the two major thrusts in southern Glacier National Park, the Lewis and the Brave Dog faults (Yin *et al*. 1989, Yin & Kelty 1991a,b), are not exposed, they are projected onto the cross-sections AA' and BB', shown in Figs. 3 and 4. The projection is based on their regional extent and stratigraphic positions as observed in southern Glacier Park (Yin & Kelty 1991a).

The most areally extensive fault in the study area, the Gunsight thrust, has flat–ramp and gently antiformal geometries. It is exposed along both the hangingwall
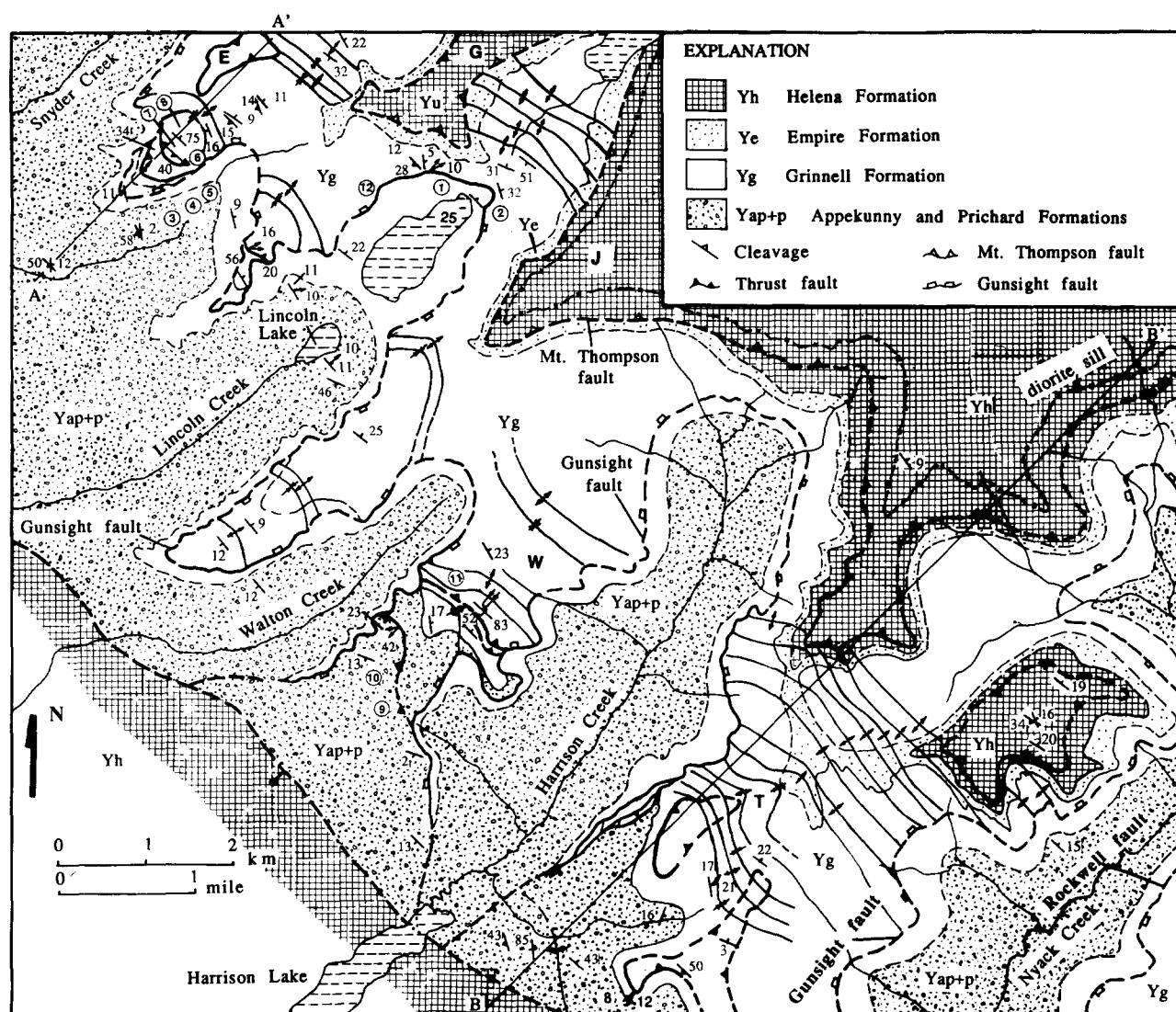
Fig. 2. Simplified geologic map of the study area and the locations of cross-sections AA' and BB' in Figs. 3 and 4. Circled numbers show the sample locations for strain measurements. E = Edwards Mountain; G = Gunsight Mountain; J = Jackson Mountain; W = Walton Mountain; T = Mount Thompson.

ramp and flat. The cut-off angle between the thrust and the footwall bedding is about 7°. The fault zone is everywhere less than 50 cm thick and consists mainly of black gouge, which is foliated so as to form a SW-dipping spaced cleavage. The fault is an NE- to ENE-directed thrust, as indicated by the offset of the Appekunny–Grinnell contact, the presence of abundant NE-dipping extensional veins and the cleavage dip in the fault zone, NE-verging folds directly above and below the fault, and NE–SW-trending striations on the fault surface. The striations are defined by both grooves and stretched quartz fibers. Slip along the fault, estimated by the offset of the Appekunny–Prichard Formation (Figs. 3 and 4), is about 3.5 km.

The Gunsight thrust is correlative with the Rockwell fault, a major low-angle bedding-parallel fault mapped in southern Glacier Park (Yin 1988, Yin & Kelty 1991a). Yin (1988) followed the Rockwell fault to exposures along the southeast side of the Nyack Creek valley (Fig. 2). This study reveals that the Gunsight thrust is exposed along the opposite side of the same valley (Fig. 2).

Because in both exposures the fault separates quartz arenite beds above from siltite beds below in the lower part of the Grinnell Formation, we interpret it as one and the same fault. Along the east side of the park the Rockwell fault is the roof fault of the Rising Wolf Mountain duplex in the Lewis thrust plate (Yin & Kelty 1991a). A kinematic model for the development of both the Rising Wolf and Brave Dog duplexes in the Lewis thrust sheet was presented by Yin et al. (1989). This model differs from the conventional duplex model of Dahlstrom (1970) and Boyer & Elliott (1982) in that the entire roof and floor thrusts operate simultaneously during the development of thrust imbricates between the two. As the Rockwell fault is kinematically linked by the duplex with its basal fault, the Lewis thrust, the two are synchronous. The correlation of the Gunsight thrust with the Rockwell fault implies that the Gunsight fault is also synchronous with the Lewis thrust. However, as thrust imbricates in the Rising Wolf Mountain duplex cut the Brave Dog fault (Yin & Kelty 1991a), the Rockwell and the Gunsight faults post-date the Brave
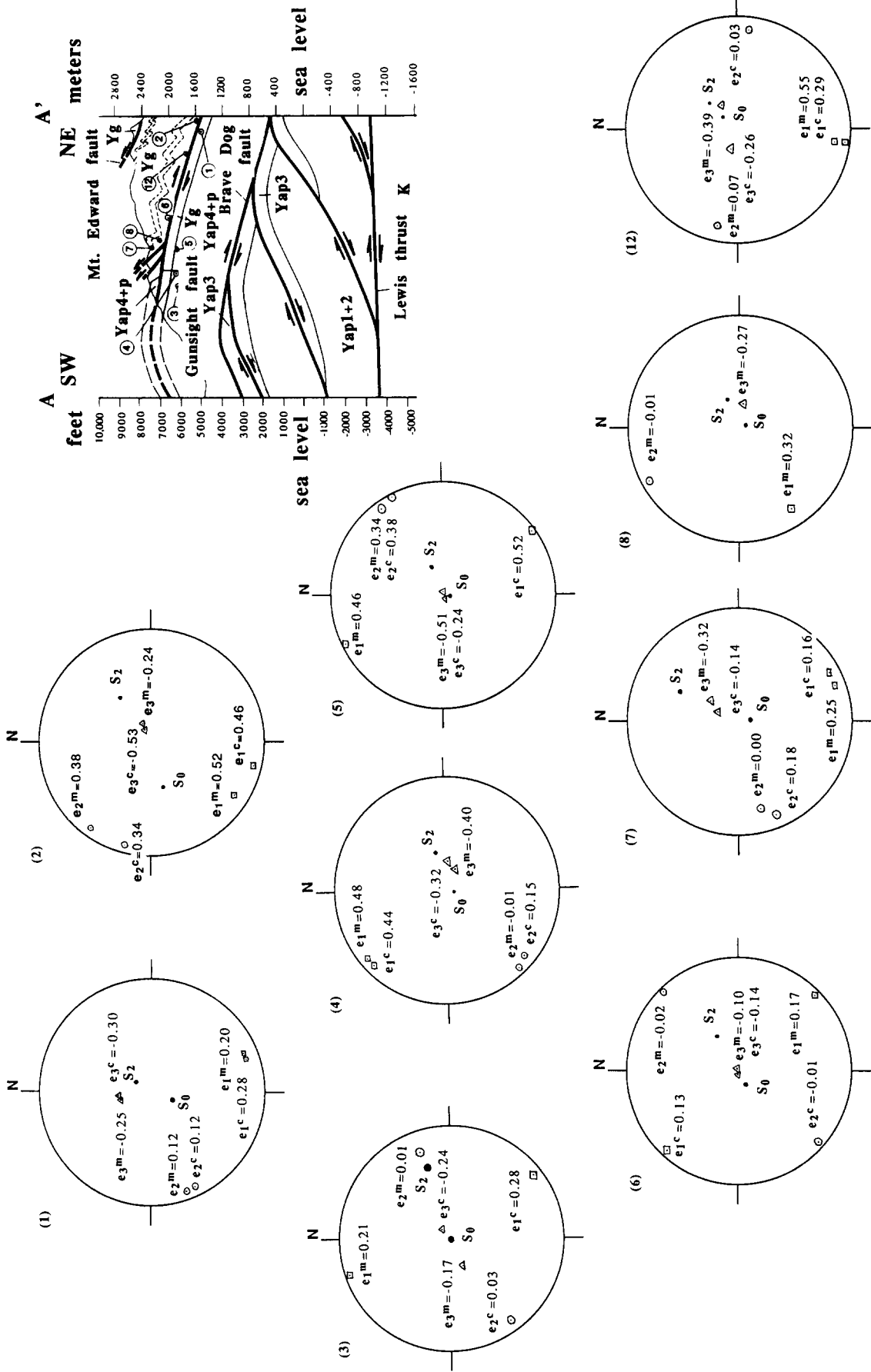
Fig. 3. Cross-section AA'. Circled numbers show the sample locations for strain measurements. Dashed lines are marker beds showing the style of folding and relation between bedding and faults. Stratigraphic units from older to younger are denoted as Yap1+2 for members 1 and 2 of the Appekunny Formation, Yap3 for member 3 of the Appekunny Formation, Yap4+p for member 4 of the Appekunny Formation and the Prichard Formation, Yg for the Grinnell Formation, and K for the Cretaceous strata. The orientations and magnitudes of the March strains are shown in stereographic projection. e_1 (squares) for the maximum elongation strain, e_2 (circles) for the intermediate elongation strain, e_3 (triangles) for the minimum elongation strain, e^m and e^c are the March strains determined by the preferred orientation of mica and chlorite, respectively. Geographic orientations of the corresponding bedding poles (S_0) and regional cleavage poles (S_2) are shown for comparison.

Dog fault (Figs. 3 and 4). This inference of age relationship among the Lewis, the Gunsight and the Brave Dog faults forms the basis for the kinematic model proposed below.

Directly above the Gunsight thrust is an E-verging anticline (Fig. 5a) with a flat to gently SW-dipping backlimb, a steeply NE-dipping forelimb, and a narrow hinge zone between them (Figs. 3 and 4). Bedding of the steep forelimb is truncated by the Gunsight thrust below (Figs. 3, 4 and 5a). The cut-off angle between the fault and the hangingwall beds ranges from 70° to 90°. The fold interlimb angle of the anticline is 120° in the northern part of the area (Fig. 4) and 90° in the southern part (Fig. 3). The Gunsight thrust does not terminate in the core of the hangingwall anticline above it; instead, it can be traced eastward to the undeformed strata where the fault parallels bedding in both its hangingwall and footwall (Figs. 3 and 4).

Both limbs of the hangingwall anticline are complexly deformed. Deformation in the forelimb is characterized by W-directed thrusts with offsets of less than 20 m and minor folds (Figs. 3 and 4). The shallow-dipping backlimb is deformed by a few E-verging overturned folds.

The total bedding-parallel shortening of the forelimb by thrusting, folding and penetrative strain is no more than 20%, because no significant change in stratigraphic thickness across the hinge of the hangingwall anticline can be detected in the field.

A 4-km wide fold belt, the frontal fold complex (Figs. 2 and 4), is present directly east of the E-verging anticline. This complex is bounded above by the Mount Thompson fault, which lies in the lower part of the Helena Formation between dominantly limestone above and interbedded limestone and quartz arenite below. The fault is parallel to the undeformed to broadly folded strata above, but is strongly discordant with the folded strata below (Fig. 5b). The average amplitude of the minor folds in the complex is 30–50 m, and fold wavelengths are 50–150 m. Folds in the western part of the complex are mostly E-verging or symmetric, whereas folds in the eastern part of the fold belt and directly below the Mount Thompson fault are W-verging (Figs. 3, 4 and 5c). The total shortening across the 4-km wide fold complex is about 1.2 km. Shortening in the fold complex, as indicated by the tightness of the folds, is most pronounced in the middle and least on both sides.
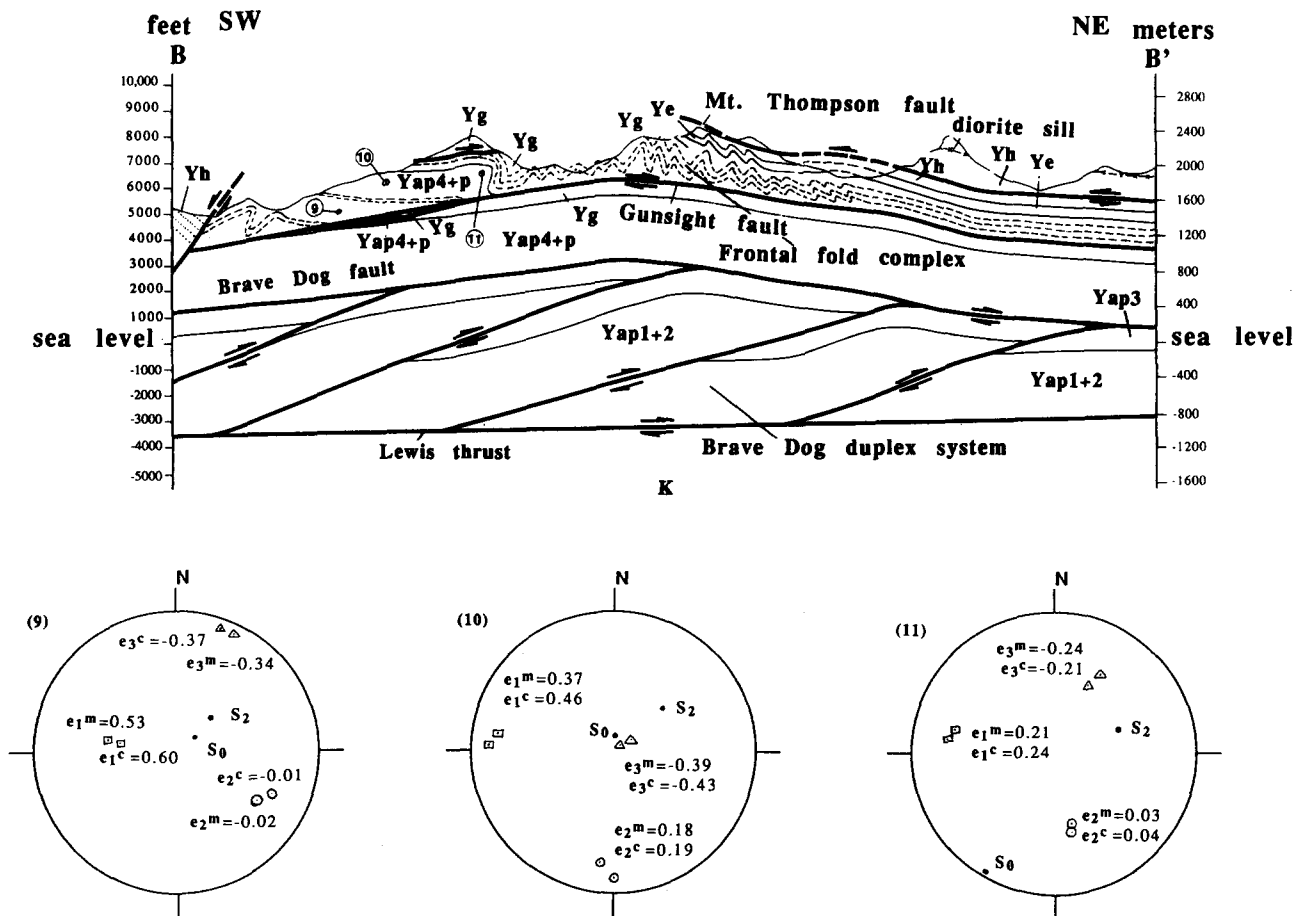

Fig. 4. Cross-section BB'. Circled numbers show the sample locations for strain measurements. Dashed lines are marker beds showing the style of folding and relation between bedding and faults. Stratigraphic units from older to younger are denoted as Yap1+2 for members 1 and 2 of the Appekunny Formation, Yap3 for member 3 of the Appekunny Formation, Yap4+p for member 4 of the Appekunny Formation and the Prichard Formation, Yg for the Grinnell Formation, Ye for the Empire Formation, Yh, for the Helena Formation, and K for the Cretaceous strata. The orientations and magnitudes of the March strains are shown in stereographic projection, e_1 (squares) for the maximum elongation strain, e_2 (circles) for the intermediate elongation strain, e_3 (triangles) for the minimum elongation strain, e^m and e^c are the March strains determined by the preferred orientation of mica and chlorite, respectively. Geographic orientations of the corresponding bedding poles (S_0) and regional cleavage poles (S_2) are shown for comparison.

The fold complex and the E-verging anticline together are enveloped by little-deformed strata above that define a single broad anticline.

Minor W-verging folds with both amplitudes and wavelengths of several meters are present directly below the Mount Thompson fault, suggesting that it is W-directed. The fault zone is excellently exposed. Like the Gunsight fault, it consists of a less than 1 m thick layer of gouge. The gouge zone is locally foliated and produces an E-dipping cleavage. Both the vergence of the minor folds and the dipping cleavage in the fault zone confirm that the fault is W-directed. The Mount Thompson fault is different from the 'passive roof fault' of Banks & Warburton (1986) because nowhere in the study area is it directly linked with the Gunsight fault to form the tip-line of a blind thrust (cf. fig. 7 of Banks & Warburton 1986). It is merely an accommodation zone or décollement separating the highly folded strata below from less folded strata above. For the same reason, the frontal fold complex does not resemble a 'triangular zone' of Price (1986).

Two sets of spaced cleavage are found in the study area (S_1 and S_2). S_1 is weakly developed and is locally present in the thinly-bedded (a few centimeters and less) argillite layers along the hinge zones of minor folds in the frontal fold complex. It is vertical to NE-dipping, depending on the vergence of the associated minor folds. S_2 is well developed, and is present in both argillite and quartz arenite beds throughout the study area. It dips everywhere southwest at angles varying from 30° to 50°. Its dip direction is thus independent of either bedding attitudes, which can be anywhere from subhorizontal to vertical, or the minor fold vergence in the frontal fold complex. A direct cross-cutting relationship between the two sets of cleavage has not been observed because outcrops with S_1 cleavage are rare. However, S_1 probably pre-dates S_2 because it is associated with the same folds in the frontal zone which are transected by SW-dipping S_2, regardless of their vergence.

The aforementioned structural association consisting of: (1) the Gunsight thrust; (2) the E-verging hanging-wall anticline; (3) the frontal fold complex; (4) the Mount Thompson fault; and (5) the W-dipping spaced cleavage is referred to as the thrust-related fold complex, because their development can be demonstrated to be related to the emplacement of the Gunsight thrust sheet.

A SW-dipping normal fault along the west side of the study area cuts all the contractional structures and can thus be interpreted as a member of the late Eocene to early Oligocene Flathead normal fault system that is fully developed a few kilometers to the west (Fig. 1) (Ross 1959, Bally et al. 1966, Dahlstrom 1970, McMechan & Price 1980, Constenius 1982, Powell et al. 1988).

STRAIN DETERMINATION

Figures 2–4 show the locations of 12 oriented samples along three traverses across the hangingwall structure,

taken to determine strain since deposition. All the samples were collected in the western part of the study area where S_1 is not observed. Directions and magnitudes of March strains (March 1932, Oertel 1983, 1985) were measured from these samples, and the spatial relationship of these strains to cleavage S_2 and bedding S_0 are shown stereographically in Figs. 3 and 4.

Methods and assumptions

Preferred orientations of mica and chlorite grains in these samples were measured on an X-ray pole-figure goniometer (Oertel 1985, Wenk 1985). We calculated the strain according to the theory of March (1932) by the procedure discussed in detail by Oertel (1983) and Oertel et al. (1989).

The March theory of strain determination from preferred orientation of platy mineral grains assumes that clay grains were originally oriented at random, either at deposition or after subsequent bioturbation. Later the clay grains develop a preferred orientation parallel to bedding as compaction proceeds and pores collapse, resulting in a pole distribution axially symmetric with respect to the bedding pole. Where a tectonic strain follows or proceeds simultaneously with compaction, clay grains rotate so that their basal planes tend to face the direction of tectonic compression. The preferred orientation thus reflects the cumulative strain from the deposition of a mudrock onward.

In the case of the Belt Supergroup, deposition occurred between about 1400 and 850 Ma (Obradovich et al. 1984). Broad folding may have affected the Belt rocks before the deposition of the Middle Cambrian sediments, as suggested by the local development of a Proterozoic cleavage in southeastern British Columbia (McMechan & Price 1982) and by the irregular unconformity between the Belt and Middle Cambrian strata (Harrison et al. 1974). Before the Mesozoic, however, the Belt rocks in northwestern Montana do not seem to have experienced any appreciable contraction or extension that can be demonstrated by the development of faults or folds. Thus, as a first approximation, the strain measured in the Belt strata of the study area is interpreted to be the result of a superposition of two processes: (1) the compaction during and immediately after the deposition of the Belt Supergroup; and (2) a late Cretaceous to early Tertiary deformation during the emplacement of the Gunsight thrust sheet. Because strain produced by compaction is characterized by being axially symmetric about the bedding pole and by having its greatest shortening axis parallel to the bedding pole, any deviation from such an expectation may be interpreted as the result of later tectonic deformation. As we know little about the magnitude of the compaction strain in this area, the following discussion of the March strain measurements is concerned mostly with the spatial variation of the principal strain axes with respect to bedding and with its relationship to the thrust transport direction.
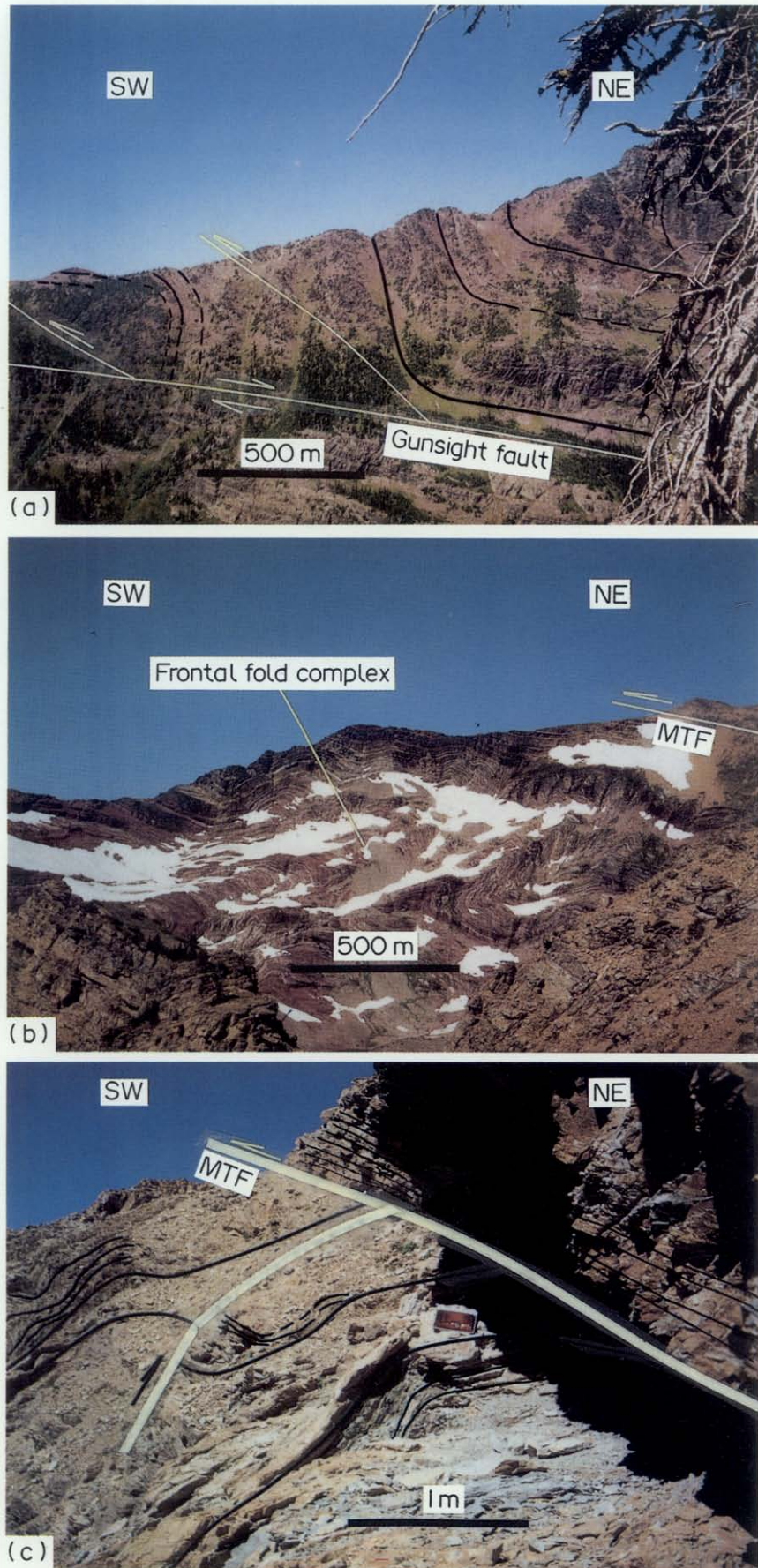
Fig. 5. (a) A hanging-wall ramp and the fault-bend fold in the hangingwall of the Gunsight thrust at Walton Mountain viewed from the southeast. (b) Frontal fold complex below the Mount Thompson roof fault on Mount Thompson, viewed from the south. (c) Mount Thompson fault and W-verging folds immediately below on Mount Thompson, viewed from the south.

713

Results of March strain measurements

The orientations of the maximum (e_1), intermediate (e_2) and minimum (e_3) principal March strains (positive for extension) and their relationships to bedding S_0 and regional cleavage S_2 are shown in Figs. 3 and 4, e^c and e^m represent strains determined from preferred orientation of chlorite and mica, respectively. The cause of the discrepancies between the measurements on the two phyllosilicates is not known; it may be taken as a measure of the uncertainty of our strain estimates. In the Mount Edward and Gunsight Mountain area in the northern study area, samples 3–5 were collected in the footwall of the Gunsight fault from the almost unfolded and unfaulted Prichard, Appekunny and Grinnell Formations (Fig. 3). Prevalent compaction strain is responsible for the subparallelism of the minimum strain direction, e_3, with the bedding pole, S_0, in all three samples. Their maximum elongation directions e_1 are consistently perpendicular to the Gunsight thrust transport direction and parallel to the NW-trending fold hinges in the hangingwall.

Strains measured within 5 m above and below the Gunsight thrust (samples 1, 2, 6 and 12 in Fig. 3) are more complex than those measured in the footwall: the maximum elongation direction is subparallel to the thrust transport direction for sample 2, subperpendicular to this direction for samples 1 and 6, and oblique to it for sample 12.

Strains measured in two samples from the steep forelimb of the E-verging hangingwall anticline near the northern cross-section AA' (samples 7 and 8 in Fig. 3) show maximum elongation direction e_1 parallel to the transport direction in one, perpendicular to it in the other. They are approximately perpendicular to the local bedding poles S_0 and thus imply both local forelimb thickening and thinning.

Strains measured in the backlimb of the hangingwall anticline near the southern section BB' (samples 9–11 in Fig. 4) all have their maximum elongation directions, e_1, parallel to the thrust transport direction and the bedding. This suggests that beds in the backlimb were stretched in the northeast direction.

The tectonic strain, as registered by the preferred orientation, cannot have been coaxial with the compaction strain. The evidence for this is the deviation of the direction of greatest shortening, e_3, from the bedding pole, S_0, at all sample localities. The angle of deviation is large enough to be clearly significant in many instances and is probably significant even where it is small, as shown by its systematic geometry. In most cases e_3 plunges less steeply than the bedding pole and lies near the great circle connecting S_0 with the generally more shallowly plunging pole of the regional cleavage S_2, thus reflecting the superposition of a tectonic greatest shortening oblique to the bedding pole onto the compaction strain. The axis of greatest tectonic compression seems to have lain in the NE quadrant of the lower hemisphere. One possible explanation is the presence of a topographic high to the southwest of the sampled rocks while they were deformed. The same high, together with the tectonic compression in the NE–SW direction may have contributed to the driving force for the Gunsight thrust. Exceptional in this respect is sample 9, in which e_3 has a much shallower northeastward plunge than the cleavage pole and lies almost at a right angle to the bedding pole; the tectonic NE–SW compression seems to have contributed more to the cumulative strain than the compaction, and the e_3 axis has become very shallow as a consequence.

At only a few of the sample localities is the S_2 pole, as measured in the field, subparallel to the direction of e_3, as determined from the preferred orientation. In most cases the discrepancy between the two directions exceeds our estimated margin of error. We explain the difference by the domainal nature of the preferred orientation in these samples.

From hand specimen inspection, the spaced S_2 cleavage seems to have been caused by stress solution of matrix material and the concomitant concentration and alignment of the less soluble phyllosilicates in the cleavage seams. A distinctive preferred orientation of phyllosilicates in the microlithons and the seams is typical for this type of cleavage, and it can be taken to reflect the local strains, strain within the seams having been more intensive than in the microlithons. The insufficient spatial resolution of the X-ray pole-figure goniometer does not allow separate determinations of the preferred phyllosilicate orientation in the seams and microlithons, and our strain estimates are based on a collective estimate of the preferred orientation in the two domain types together. The seams, however, form only a small volumetric proportion of the rock, and generally the X-ray beam strikes only, or mostly, microlithon material. It thus registers predominantly the cumulative strain undergone by this material before the cleavage formation, possibly with an additional increment while solution–precipitation processes were active in the seams. This addition should have been small, considering that the seams were probably the most easily deformable portion of the rock while stress solution was active.

Because phyllosilicates are more highly concentrated in the seams than in the microlithons, and because they necessarily have a higher degree of preferred orientation, sampling by the X-ray beam of even volumetrically small portions of seam material affects the measured integrated preferred orientation strongly. In slates with regularly and closely spaced cleavage seams, the X-ray beam samples both, and the integrated preferred orientation of the two together gives an adequate measure of the mean strain. This does not appear to be the case for all samples in this study, because seams in the sampled rocks are widely spaced, and their average spacing varies locally.
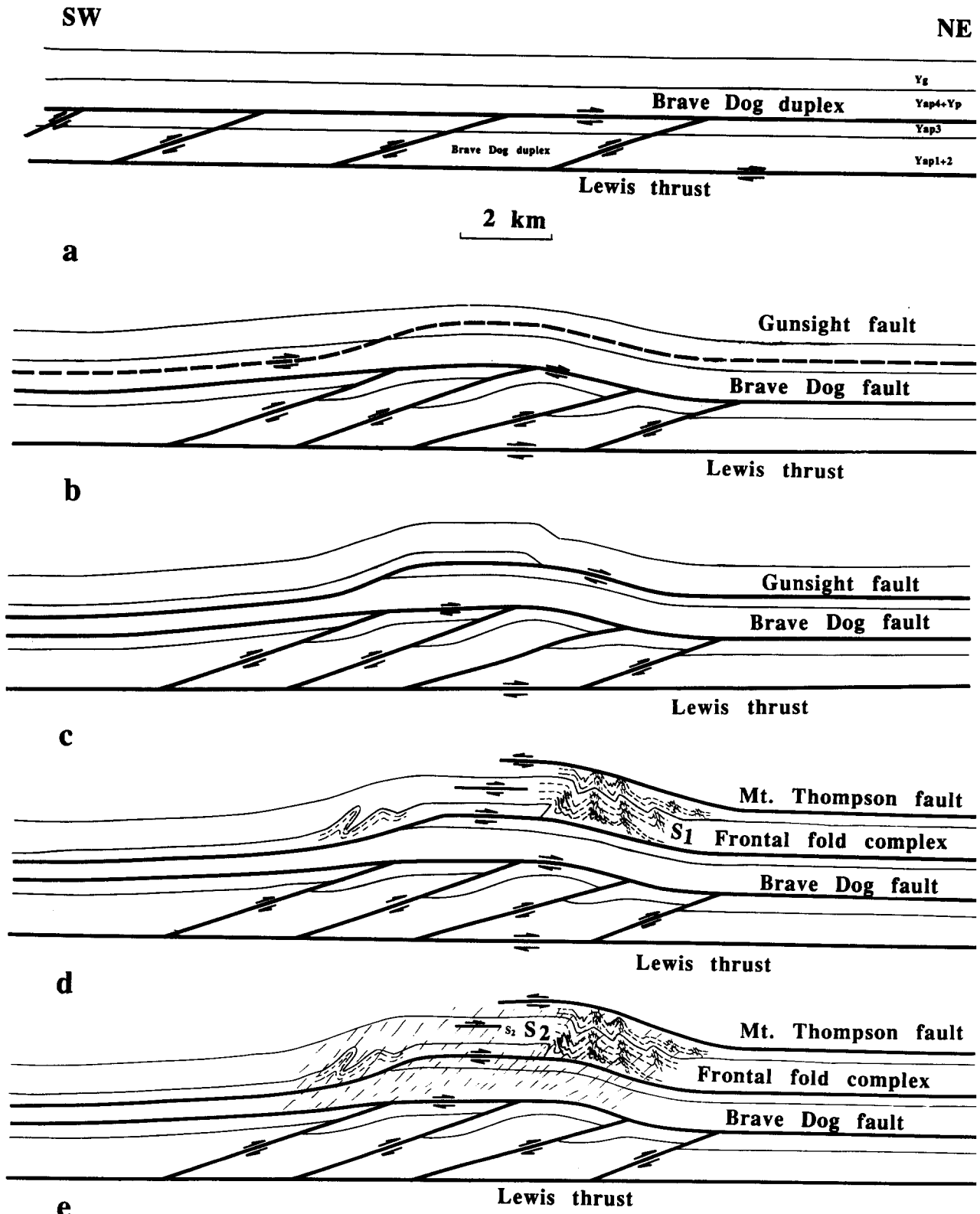
Fig. 6. Kinematic model for the development of fault-bend fold in west-central Glacier National Park, Montana. (a) Initiation and development of the Brave Dog duplex between Lewis thrust and Brave Dog fault. Yap1+2 for members 1 and 2 of the Appekunny Formation, Yap3 for member 3 of the Appekunny Formation, Yap4+p for member 4 of the Appekunny Formation and the Prichard Formation, and Yg for the Grinnell Formation. (b) Initiation of the Gunsight thrust above the antiformal Brave Dog fault. (c) Emplacement of the Gunsight thrust plate and development of the fault-bend fold as a consequence of motion along the Gunsight fault flat–ramp. (d) Formation of the hangingwall anticline and development of the frontal fold complex. Local top-to-the-west bedding-parallel shearing causing development of W-verging folds in the frontal fold complex and initiation of the W-directed Mount Thompson fault. NE–SW bedding-parallel shortening in the footwall and extension in the hangingwall as the anticlinal fault-bend fold develops further. Development of local E-dipping cleavage S_1 along the hinge zones with tightening of the W-verging folds in the frontal complex. (e) Development of W-dipping, regional cleavage S_2.

DISCUSSION

Kinematic origin of the asymmetric hangingwall anticline

The E-verging hangingwall anticline above the Gunsight thrust exhibits the geometry of a fault-bend fold (Rich 1934). It could thus have developed according to the kinematic model of Suppe (1983). However, when the model is applied assuming constant bed thickness during folding (equation 12 in Suppe 1983) and using the observed initial cut-off angle (7°), the predicted interlimb angle (2γ) of the anticline and the final cut-off angle (β) are 176° and 8° for the mode I fold and 20° and 160° for the mode II fold. However, the observed interlimb and final cut-off angles, $2\gamma = 90$–$120°$ and $\beta = 70$–$90°$, are both inconsistent with the model. Considering uniform forelimb thickening and applying Jamison's fault-bend fold model (fig. 3 of Jamison 1987), no solution exists for observed interlimb angles of 90–120° and an initial cut-off angle of 7°, no matter how much forelimb thickening one assumes. It is, however, conceivable that the fold originated from an initial, open mode I fault-bend fold, and that the observed interlimb angle of 90–120° resulted from later tightening of the fold. The presence of E-directed bedding-parallel faults in the backlimb and of W-directed steep thrusts in the forelimb (Figs. 3 and 4) is consistent with flexural-slip in the anticline as it was tightened. In addition, the southward increase in the tightness of the hangingwall anticline (cf. AA' and BB' in Figs. 3 and 4) may also be the result of progressive tightening.

An apparent Rich-type fault-bend fold (Rich 1934) can also be the result of fault-propagation folding because the two types of fold share many geometric features (Jamison 1987, Mitra 1990, Suppe & Medwedeff 1990). However, applying Jamison's fault-propagation model (fig. 2 of Jamison 1987) together with forelimb thickening, we again found no solution for the observed interlimb angles of 90–120° starting from an initial cut-off angle of 7°. With 20% forelimb thickening strain, the predicted fold interlimb angle is about 10°, much tighter than observed. It seems unlikely that the observed angle of 90–120° resulted from reopening a tight fold from an initial interlimb angle of 10°, because, contrary to observations, this would require flexural W-verging folding and thrusting in the backlimb and E-verging features in the forelimb.

The poor fit of the observed geometry with all constant-volume balanced cross-section models could be due to significant volume loss during or after the folding. The widespread spaced cleavage could well have been the result of volume loss by stress solution.

The geometry of the entire thrust-related fold system differs from either a fault-bend fold or a fault-propagation fold by possessing (1) a passive roof fault that transports in the direction opposite to that of the basal thrust, and (2) a complexly deformed fold zone in front of an asymmetric hangingwall anticline between the basal thrust and the roof fault. The development of the Mount Thompson roof fault caused the disharmony of folding above and below.

Strain in a fault-related fold complex

The strain in the hangingwall of a thrust is necessarily influenced by its emplacement history, the folding style, and the shape of the underlying thrust surface. As discussed by Evans & Dunne (1991), different stages of thrust emplacement produce distinct strain patterns in the hangingwall. Jamison (1987) discussed the geometric and kinematic consequences of forelimb thickening and thinning for cross-section balancing. Cooper & Trayner (1986) pointed out that hangingwall structures can significantly differ depending on whether they were emplaced along a planar surface, which favors development of a hinterland-dipping cleavage, or along a staircase surface, which favors backthrusting. In none of those models, however, was the possibility considered that bedding-parallel extension in the thrust transport direction could occur along the backlimb of a fault-bend fold, where our study found it to dominate. It was probably caused by the bending induced during the tightening of the anticline and its emplacement across the Gunsight thrust ramp. As shown by Wiltschko (1981), directly above a thrust ramp bending of a viscous thrust sheet can cause tensile stress in the transport direction.

Complex strain, like that adjacent to the Gunsight fault zone with both extension and shortening parallel to the thrust transport direction, has been documented by numerous workers in fault zones near other major thrusts by the presence of mesoscopic contractional and extensional faults (e.g. Platt & Leggett 1986, Wojtal 1986, Wojtal & Mitra 1986, 1988, Yin & Kelty 1991a). Platt & Leggett (1986) attributed local secondary extensional and contractional faults in the Makaran accretionary prism of southwestern Pakistan to variations of the sliding friction along a primary thrust. In particular, they proposed that a region of high friction can lead to extension and contraction in both hangingwall and footwall in an antisymmetric fashion. On the basis of their extensive studies of the Appalachian thrusts, Wojtal & Mitra (1986, 1988) interpreted extensional and contractional faults as the result of episodic alternations of strain hardening and softening during the evolution of a thrust frault zone. Yin & Kelty (1991a) explained such faults along the base of the Lewis thrust sheet as Riedel and primary shear planes formed during an overall simple-shear deformation. Thus instantaneous elongation parallel to the transport direction near a thrust is plausible. However, it is difficult to determine which of the invoked mechanisms may have been responsible for the observed strain field near the Gunsight thrust. Loci of high-friction or of strain-hardening may have varied both spatially along the fault zone and temporally through the course of its evolution, and our observations allow no unambiguous assignment of any particular sequence or particular local distribution of

domains in which deformation was governed by one or the other of these mechanisms.

KINEMATIC MODEL

The structural relations in our study area provide the basis for a kinematic model (Fig. 6). Emplacement of the Lewis thrust sheet started with the initiation and development of the Brave Dog duplex between the Lewis and the antiformal Brave Dog faults (Figs. 6a & b). The development of the Brave Dog fault was followed by the initiation, above it, of the Gunsight thrust in the anticlinal Grinnell Formation (Fig. 6b). We speculate that the Gunsight thrust ramp was localized by the presence of the anticline, produced in turn by the Brave Dog duplex. Because this is a gentle warp of only a few degrees on either limb, less energy may have been expended by the Gunsight thrust following the curved bedding plane than would have been needed to cut bedding along a new, straight fault segment. The E-verging hangingwall anticline above the Gunsight fault could have been initiated as an open fault-bend fold (Fig. 6c). Further emplacement of the Gunsight plate caused both the development of the frontal fold complex and the tightening of the hangingwall anticline (Fig. 6d). Associated with the latter are the development of E-directed flat faults in the backlimb and W-directed thrusts in the forelimb. The backlimb was stretched as it passed the thrust ramp. The top-to-the-west bedding-parallel Mount Thompson fault was initiated as a consequence of the piling up of the frontal fold complex (Fig. 6d). Further fold tightening in this complex led to the formation of the cleavage S_1 in hinge zones (Fig. 6d). During or after the emplacement of the Gunsight thrust sheet the regional, W-dipping cleavage S_2 developed (Fig. 6e).

CONCLUSIONS

(1) The thrust-related fold system described in this study differs geometrically from both a fault-bend and a fault-propagation fold in that it possesses (1) a passive roof fault that transported in the direction opposite to that of the basal thrust, and (2) a complexly deformed fold zone that was developed in front of an asymmetric hangingwall anticline and lies between the basal thrust (the Gunsight fault) and the roof fault (the Mount Thompson fault). The development of the Mount Thompson fault led to the disharmonic geometry of strata above and below it.

(2) The present geometry of the hangingwall anticline in the thrust-related fold complex, specifically the observed initial cut-off angle and the fold interlimb angle, cannot be explained by balanced cross-section models. It is geometrically possible, however, that the anticline was initiated as an open fault-bend fold and was later tightened during its eastward emplacement. Alternatively, the poor fit of the observed fold geometry to

balanced cross-section models could be due to significant volume loss during and after the formation of the hangingwall anticline.

(3) The principal directions and magnitudes of strain in the fault-related fold system vary from place to place. The forelimb of the hangingwall anticline exhibits both bedding-parallel thinning and thickening. The backlimb of the hangingwall anticline underwent bedding-parallel stretching in the thrust transport direction. Adjacent to the Gunsight thrust, strain in the thrust transport direction was either shortening or extension. Such a strain field may be caused by inhomogeneous friction along the fault surface, or by an alternation of strain hardening and softening during the evolution of the basal thrust fault zone.

REFERENCES

Bally, A. W., Gordy, P. L. & Stewart, G. A. 1966. Structure, seismic data, and orogenic evolution of southern Canadian Rockies. *Bull. Can. Petrol. Geol.* **14**, 337–381.

Banks, C. J. & Warburton, J. 1986. "Passive roof" duplex geometry in the frontal structures of the Kirhar and Sulaiman mountain belt, Pakistan. *J. Struct. Geol.* **8**, 229–238.

Boyer, S. M. & Elliott, D. W. 1982. Thrust systems. *Bull. Am. Ass. Petrol. Geol.* **66**, 1196–1230.

Constenius, K. 1982. Relationship between the Kishenehn Basin, and the Flathead listric normal fault system and the Lewis thrust salient. In: *Geologic Studies of the Cordilleran Thrust Belt* (edited by Powers, R. B.). *Rocky Mountain Geologists* **20**, 817–830.

Cooper, M. A. & Trayner, P. M. 1986. Thrust surface geometry: implications for thrust-belt evolution and section-balancing techniques. *J. Struct. Geol.* **8**, 305–312.

Dahlstrom, C. D. A. 1970. Structural geology in the eastern margin of the Canadian Rocky Mountains. *Bull. Can. Petrol. Geol.* **18**, 332–406.

Davis, G. A. & Jardine, E. A. 1984. Preliminary studies of the geometry and kinematics of the Lewis allochthon, Saint Mary Lake to Yellow Mountain, Glacier National Park, Montana. *Montana Geol. Soc.* 1984 *Field Conf. Guidebook*, 201–209.

Erslev, E. A. 1991. Trishear fault-propagation folding. *Geology* **19**, 717–720.

Evans, M. A. & Dunne, W. M. 1991. Strain factorization and partitioning in the North Mountain thrust sheet, central Appalachians, U.S.A. *J. Struct. Geol.* **13**, 21–35.

Gordy, P. L., Frey, F. R. & Norris, D. K. 1977. Geological guide for the C.S.P.G. 1977 Waterton-Glacier Park field conference. *Can. Soc. Petrol. Geol.*

Harrison, J. E., Griggs, A. B. & Wells, J. D. 1974. Tectonic features of the Precambrian Belt Basin and their influence on post-Belt structures. *Prof. Pap. U.S. geol. Surv.* **866**, 1–15.

Hudec, M. R. 1986. Geology of a portion of the Lewis thrust plate north of Two Medicine Lake, Glacier National Park, Montana. Unpublished M.S. thesis, University of Southern California, Los Angeles, California.

Hudec, M. R. & Davis, G. A. 1989. Out-of-sequence thrust faulting and duplex formation in the Lewis thrust system, Spot Mountain, southeastern Glacier National Park, Montana. *Can. J. Earth Sci.* **26**, 2356–2364.

Jamison, W. R. 1987. Geometric analysis of fold development in overthrust terranes. *J. Struct. Geol.* **9**, 207–219.

Jardine, E. A. 1985. Structural geology along a portion of the Lewis thrust fault. Unpublished M.S. thesis, University of Southern California, Los Angeles, California.

Kelty, T. K. 1985. The structural geology of a portion of the Lewis thrust plate, Marias Pass, Glacier National Park, Montana. Unpublished M.S. thesis, University of Southern California, Los Angeles, California.

March, A. 1932. Mathematische Theorie der Regelung nach der Korngestalt bei affiner Deformation. Z. Kristallogr. 81, 285–297.

McGimsey, D. H. 1979. Structural Geology of the Wolf Gun Mountain area, Glacier National Park, Montana. Unpublished M.S. thesis, University of Colorado, Boulder, Colorado.

McMechan, R. D. & Price, R. A. 1980. Reappraisal of reported unconformity in the Paleogene (Oligocene) Kishenehn Formation: Implications for Cenozoic tectonics in the Flathead valley graben, southeastern British Columbia. Bull. Can Petrol. Geol. 28, 37–45.

McMechan, R. D. & Price, R. A. 1982. Superimposed low-grade metamorphism in the Mount Fisher area, southeastern British Columbia—Implications for the East Kootenay orogeny. Can. J. Earth. Sci. 19, 476–489.

Mitra, S. 1990. Fault-propagation folds: Geometry, kinematic evolution, and hydrocarbon traps. Bull. Am. Ass. Petrol. Geol. 74, 921–945.

Mudge, M. R. 1982. A resume of the structural geology of Northern Disturbed Belt, northwestern Montana. In: Geologic Studies of the Cordilleran Thrust Belt (edited by Powers, R. B.). Rocky Mountain Ass. Geol. 20, 91–122.

Mudge, M. R. & Earhart, R. L. 1980. The Lewis thrust fault and related structures in the disturbed belt, northwestern Montana. Prof. Pap. U.S. geol. Surv. 1174, 1–18.

Obradovich, J. D., Zartman, S. E. & Peterman, Z. E. 1984. Update of the Geochronology of the Belt Supergroup. In: Belt Symposium II (edited by Hobbs, S. W.). Spec. Publ. Montana Bureaau Mines & Geol. 90, 82–84.

Oertel, G. 1983. The relationship of strain and preferred orientation of phyllosilicate grains in rocks—A review. Tectonophysics 100, 413–447.

Oertel, G. 1985. Reorientation due to grain shape. In: Preferred Orientation in Deformed Models and Rocks: An Introduction to Modern Texure Analysis (edited by Wenk, H.-R.). Academic Press, San Diego, 259–265.

Oertel, G., Engelder, T. & Evans, K. 1989. A comparison of the strain of crincoid columnals with that of their enclosing silty and shaly matrix on the Appalachian Plateau, New York. J. Struct. Geol. 11, 975–993.

Platt, J. P. & Leggett, J. K. 1986. Stratal extension in thrust footwalls, Makaran accretionary prisim: Implications for thrust tectonics. Bull. Am. Ass. Petrol. Geol. 70, 191–203.

Powell, C. M., Williams, G. D. & Seagord, R. D. 1988. Using preexisting cleavage to define extensional fault geometry: an example from Glacier National Park, Montana. Geology 16, 878–880.

Price, R. A. 1981. The Cordilleran foreland thrust and fold belt in the southern Canadian Rocky Mountains. In: Thrust and Nappe Tectonics (edited by McClay, K. & Price, N. J.). Spec. Publs. geol. Soc. Lond. 9, 427–446.

Price, R. A. 1986. The southeastern Canadian Cordillera; thrust faulting, tectonic wedging, and delamination of the lithosphere. J. Struct. Geol. 8, 239–254.

Rich. J. L. 1934. Mechanics of low-angle overthrust faulting as illustrated by Cumberland thrust block, Virginia, Kentucky, Tennessee. Bull. Am. Ass. Petrol. Geol. 18, 1584–1596.

Ross, C. P. 1959. Geology of Glacier National Park and Flathead region, northwestern Montana. Prof. Pap. U.S. geol. Surv. 296, 1–125.

Suppe, J. 1980. A retrodeformable cross-section of northern Taiwan. Proc. geol. Soc. China 23, 46–55.

Suppe, J. 1983. Geometry and kinematics of fault-bend folding. Am. J. Sci. 283, 684–721.

Suppe, J. & Medwedeff, D. A. 1990. Geometry and kinematics of fault-propagation folding. Eclog. geol. Helv. 83, 409–454.

Suppe, J. & Namson, J. 1979. Fault-bend origin of frontal folds of the western Taiwan fold and-thrust belt. Petrol. Geol. Taiwan 16, 1–18.

Wenk, H.-R. 1985. Measurement of pole figures. In: Preferred Orientation in Deformed Models and Rocks: An Introduction to Modern Texture Analysis (edited by Wenk, H.-R.). Academic Press, San Diego, 11–47.

Whipple, J. W., Connor, J. J., Raup, O. B. & McGimsey, R. G. 1984. Preliminary report on stratigraphy of the Belt Supergroup, Glacier National Park and adjacent Whitefish Range, Montana. Montana Geol. Soc. 1984 Field Conf. Guidebook, 33–50.

Wiltschko, D. V. 1981. Thrust sheet deformation at a ramp: summary and extensions of an earlier model. In: Thrust and Nappe Tectonics (edited by McClay, K. & Price, N. J.). Spec. Publs. geol. Soc. Lond. 9, 55–63.

Wojtal, S. 1986. Deformation within foreland thrust sheets by populations of minor faults. J. Struct. Geol. 8, 341–360.

Wojtal, S. & Mitra, G. 1986. Strain hardening and strain softening in fault zones from foreland thrusts. Bull. geol. Soc. Am. 97, 674–687.

Wojtal, S. & Mitra, G. 1988. Nature of deformation in some fault rocks from Appalachian thrusts. In: Geometries and Mechanisms of Thrusting with Special Reference to the Appalatians (edited by Mitra, G. & Wojtal, S.). Spec. Pap. geol. Soc. Am. 222, 17–33.

Yin, A. 1988. Structural geology of the Lewis allochthon in a transact from Head Mountain to Peril Peak, southern Glacier National Park, Montana. Unpublished Ph.D. thesis, University of Southern California, Los Angeles, California.

Yin, A. 1991. Complex Pre-Lewis thrust deformation, southeastern Glacier Park, Montana. Mountain Geologist 28, 91–103.

Yin, A. & Davis, G. A. 1988. Complex deformation of the Lewis allochthon before the formation of the present Lewis thrust, SE Glacier National Park, Montana. Geol. Soc. Am. Abs. w. Prog. 20, 268.

Yin, A., Fillipone, J., Zarn, C., Allen, A. & Kelty, T. K. 1990. Formation of broad folds by multiple duplexes and fault-bend folds in the Lewis allochthon: Implications for crustal thickening in the cordilleran hinterland. Geol. Soc. Am. Abs. w. Prog. 22, 96.

Yin, A. & Kelty, T. K. 1991a. Structural evolution of the Lewis plate in Glacier National Park, Montana: Implications for regional tectonic development. Bull. geol. Soc. Am. 103, 1073–1089.

Yin, A. & Kelty, T. K. 1991b. Development of normal faults during emplacement of a thrust sheet: an example from the Lewis allochthon, Glacier National Park, Montana. J. Struct. Geol. 13, 37–47.

Yin, A., Kelty, T. K. & Davis, G. A. 1989. Duplex development and abandonment during the evolution of the Lewis thrust system. Geology 17, 806–810.

Yoos, T. R., Potter, C. J., Thigpen, J. L. & Brown, L. D. 1991. The Cordilleran foreland thrust belt in northwestern Montana and northern Idaho from COCORP and industry seismic reflection data. Bull. Am. Ass. Petrol. Geol. 75, 1089–1106.

Zarn, C. 1991. Geology of the Lewis allochthon, west-central Glacier National Park, Montana. Unpublished M.S. thesis, University of California, Los Angeles, California.